

Synthesis of thiolato bridged dimeric rhodium(III) triphenylphosphine complex via C–S bond cleavage: X-ray structure, DFT computation and catalytic evaluation towards transfer hydrogenation of ketones

Puspender Roy ^{a, b}, Rahul Naskar ^a, Chandan Kumar Manna ^a, Tapan Kumar Mondal ^{a,*}

^a Department of Chemistry, Jadavpur University, Kolkata, 700032, India

^b Department of Chemistry, Netaji Nagar Day College, University of Calcutta, Kolkata, 700092, India



ARTICLE INFO

Article history:

Received 16 April 2019

Received in revised form

31 July 2019

Accepted 14 August 2019

Available online xxx

Keywords:

Dimeric rhodium(III) complex

C–S bond cleavage

Transfer hydrogenation of ketones

DFT calculation

ABSTRACT

Herein, we have synthesized a new dimeric rhodium(III) triphenylphosphine complex, $[\text{Rh}_2(\text{PPh}_3)_2(\text{L})_2\text{Cl}_2]$ (**1**) via $\text{sp}^3(\text{C})-\text{S}$ bond cleavage of a thioether containing ligand, 1-(((2-(ethylthio)phenyl)diazetyl)methyl)naphthalen-2-ol ($\text{L}-\text{CH}_2\text{CH}_3$). The complex was thoroughly characterized by using various spectroscopic techniques. Dimeric structure with distorted octahedral geometry of each of the rhodium center is confirmed by single crystal X-ray diffraction method. Catalytic efficiency of the complex towards transfer hydrogenation of ketones is studied in *i*-PrOH. Electronic structure and UV–vis spectrum of the complex are interpreted by DFT and TDDFT computations.

© 2019 Elsevier B.V. All rights reserved.

1. Introduction

Transition metal mediated C–S bond activation, cleavage and transformation reactions are extensively studied for the last few decades owing to their importance in petroleum industry [1–3], synthetic chemistry [4–6], biorganic and bioinorganic chemistry [7–10]. The ligand systems played a crucial role in the metal catalyzed C–S bond activation. For desired reactivity, the binding affinity and the size of the ligands, electron density and steric factors of the ligands are tuned in the complexes [11,12]. More and more attentions are given to this research topic to explore convenient and efficient strategy. Recently, Majumdar et al. are extensively studied the iron and cobalt mediated C–S bond activation reactions and explored their chemical reactivity [13–15]. Hosoya et al. are reported the metal catalyzed selective aromatic C–S bond cleavage triggered transformations of thioarenes [16]. Shi et al. have successfully utilized rhodium catalyzed C–S bond activation to construct C–C bond [17]. Liebeskind and co-workers have reported the palladium and copper catalyzed cross coupling reactions via C–S bond cleavage reactions [18–20].

The transfer hydrogenation of ketones to the corresponding

alcohols has received considerable attention in chemical research because of its capacity to hydrogenate substrates in mild conditions [21–23] and avoids the use of high pressure vessels and compressed H₂ or moisture-sensitive hydride reagents [24–27]. People are deeply engaged to develop new catalysts for future industrial applications in terms of selectivity, efficiency, scope, simplicity and economic viability [28–31]. In our continued efforts to design and synthesis of platinum group metal complexes and to explore their catalytic activity towards transfer hydrogenation of ketones [32–35] herein, we have synthesized a new dimeric rhodium(III) triphenylphosphine complex, $[\text{Rh}_2(\text{PPh}_3)_2(\text{L})_2\text{Cl}_2]$ (**1**) via C–S bond cleavage of a thioether containing ligand, 1-(((2-(ethylthio)phenyl)diazetyl)methyl)naphthalen-2-ol ($\text{L}-\text{CH}_2\text{CH}_3$). The coordination chemistry of Pd(II) and Pt(II) with $\text{L}-\text{CH}_2\text{CH}_3$ was explored previously [36,37]. Recently, rhodium and iridium assisted $\text{sp}^2(\text{C})-\text{S}$ bond cleavage and formation of cyclometalated complexes were reported by S. Acharya et al. [38]. In the present work we have synthesized the dimeric Rh(III) complex by $\text{sp}^3(\text{C})-\text{S}$ bond cleavage of $\text{L}-\text{CH}_2\text{CH}_3$. Moreover, the catalytic efficiency of the complex towards transfer hydrogenation of ketones is studied in *i*-PrOH. Structure of the complex is confirmed by single crystal X-ray diffraction method. Electronic structure of the complex is interpreted by DFT computations.

* Corresponding author.

E-mail address: tapank.mondal@jadavpuruniversity.in (T.K. Mondal).

2. Experimental

2.1. Material and methods

Ligand, L-CH₂CH₃ was synthesized following the reported method [36]. 2-Aminothiophenol and [Rh(PPh₃)₃Cl] were purchased from Sigma Aldrich. Other chemicals and solvents were reagent grade and used as received. For spectroscopic studies HPLC grade solvents were used. Microanalyses (C, H, N) data were obtained using a PerkinElmer Series-II CHN-2400 CHNS/O elemental analyzer. Electronic spectra were measured on a Lambda 750 PerkinElmer spectrophotometer in the range 250–900 nm in acetonitrile. IR spectra were recorded as KBr pellets on a RX-1 PerkinElmer spectrometer in the range of 400–4000 cm⁻¹. ¹H NMR spectrum was taken on a Bruker (AC) 300 MHz FT-NMR spectrometer in CDCl₃.

2.2. Synthesis of [Rh₂(PPh₃)₂(L)₂Cl₂] (1)

Rh(PPh₃)₃Cl (0.380 g, 0.4 mmol) was dissolved in 20 mL of acetonitrile. To it 10 mL acetonitrile solution of L-CH₂CH₃ (0.124 g, 0.4 mmol) was added and the reaction mixture was refluxed for 8 h under N₂ atmosphere. The reaction mixture was cooled and the solvent was removed under reduced pressure. The crude product was purified by column chromatography using a silica gel (mesh 60–120). A pink coloured band of the complex (**1**) was eluted by 50% (v/v) ethyl acetate-petroleum ether solvent mixture. The solvent was removed under reduced pressure the pure complex **1** was obtained as a pink solid which was further dried under vacuum. Yield was, 0.205 g, 70%.

Anal. Calc. for C₆₈H₅₀Cl₂N₄O₂P₂Rh₂S₂ (**1**): C, 60.14; H, 3.71; N, 4.13; Found: C, 59.92; H, 3.65; N, 4.03; IR data (KBr, cm⁻¹): 747, 688, 512 (coordinated PPh₃), 1404 ν(N=N). ¹H NMR data (CDCl₃, ppm): 7.24 (PPh₃), 7.04–8.23 (other aromatic protons). UV–Vis (in acetonitrile), λ_{max} (nm) (ε × 10⁻³, mol⁻¹cm⁻¹): 320(19.55), 371(16.49), 422(sh), 515(7.43), 595(12.54).

2.3. Crystallography

Single crystals of [Rh₂(PPh₃)₂(L)₂Cl₂] (**1**) were grown by slow diffusion of n-hexane into dichloromethane solution of the complex. Single crystal data were collected using the ω scan technique with an automated Bruker SMART APEX CCD diffractometer using graphite monochromated MoKα radiation (λ = 0.71073 Å) at room temperature. Selected data collection parameters and other crystallographic results are summarized in Table 1. Reflection data were recorded using the ω scan technique. The structure was solved by direct methods and refined by full-matrix least-squares on F² techniques with anisotropic displacement parameters for all non-hydrogen atoms using SHELXL-97 [39]. The absorption corrections were done by multi-scan (SHELXTL program package) and all the data were corrected for Lorentz, polarization effect. Hydrogen atoms were included in the refinement process as per the riding model.

2.4. Computational method

Gas phase geometry of [Rh₂(PPh₃)₂(L)₂Cl₂] (**1**) was fully optimized without any symmetry constraints in singlet ground-state by DFT/B3LYP [40,41] method. For rhodium atom LanL2DZ basis set with effective core potential was employed [42–44]. For all elements 6-31 + G(d) basis set was used. The vibrational frequency calculation was performed to ensure that the optimized geometry represents real minimum of the ground state potential energy surface. Electronic spectrum was computed using the time-

Table 1

Crystallographic data and refinement parameters of [Rh₂(PPh₃)₂(L)₂Cl₂] (**1**).

Formula	C ₇₀ H ₅₄ Cl ₆ N ₄ O ₂ P ₂ Rh ₂ S ₂
Formula Weight	1527.75
Crystal System	Monoclinic
Space group	C2/c
a, b, c [Å]	23.9738(14), 9.6124(5), 30.0374(16)
α	90
β	109.396(4)
γ	90
V [Å ³]	6529.1(6)
Z	4
D(calc) [g/cm ³]	1.554
μ(MoKα) [μm]	0.914
F(000)	3088
Absorption Correction	multi-scan
Temperature (K)	296(2)
Radiation [Å]	0.71073
θ(Min-Max) [°]	1.44–25.00
Dataset (h; k; l)	−28 and 28; −11 and 11; −36 and 35
Refns collected/Unique refns/R(int)	36061/5619/0.1158
Observed data (I > 2σ(I))	2762
Data/restraints/parameters	5619/0/397
R1 ^a , wR2 ^b (I > 2σ(I))	0.0819, 0.1398
GOF ^c	1.061
Largest diff. peak/hole/e Å ^{−3}	1.460/−0.854

^a R₁ = ∑ |(F₀ − |F_c|)|/|F₀|.

^b wR₂ = { ∑ [w(F₀² − F_c²)²]/| ∑ [w(F₀²)²] } }^{1/2}, w = 1/[σ²(F₀²) + (0.0357P)² + 25.2136P], where P = (F₀² + 2F_c²)/3.

^c GOF = { ∑ [w(F₀² − F_c²)²]/(n−p) } }^{1/2}, where n = number of measured data and p = number of parameters.

dependent density functional theory (TDDFT) formalism [44–47] and the solvent effect (acetonitrile) was simulated using the conductor-like polarizable continuum model (CPCM) [48–50]. All computations were carried out using the Gaussian09 (G09) program [51]. GaussSum [52] program was used to calculate the fractional contributions of various groups to each molecular orbital for **1**.

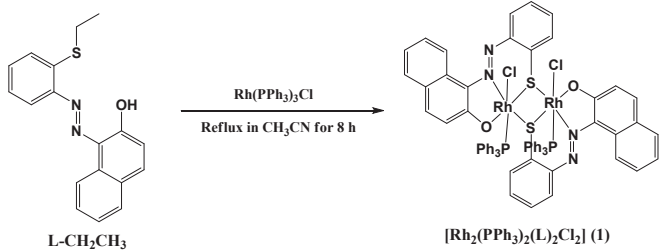
2.5. General procedure for the transfer hydrogenation of ketones

In a typical transfer hydrogenation reaction a solution complex **1** (0.004 mmol), KOH (0.02 mmol) and the corresponding ketone (2 mmol) was dissolved in 10 mL i-PrOH. The reaction mixture was degassed and refluxed at 80 °C under stirring condition. The reaction was monitored at various time intervals by GC using authentic sample. After the completion of the reaction, i-PrOH was removed under reduced pressure and extracted with diethyl ether. The conversion was determined by GC equipped with a flame ionization detector (FID) and HP-5 column of 30 m length, 0.53 mm diameter and 5.00 μm film thickness. The column, injector and detector temperatures were 200, 250 and 250 °C respectively. The carrier gas was N₂ (UHP grade) at a flow rate of 30 mL/min. The injection volume of sample was 2 μL. The alcohols were identified by GC using undecane as an internal standard and each of the catalytic run was performed three times.

3. Results and discussion

3.1. Synthesis and spectral characterization

The dimeric rhodium(III) triphenylphosphine complex, [Rh₂(PPh₃)₂(L)₂Cl₂] (**1**) was synthesized by the reaction of Rh(PPh₃)₃Cl and azo-thioether ligand, L- SCH₂CH₃ under refluxing condition in acetonitrile (Scheme 1). The complex was thoroughly characterized by several spectroscopic techniques. IR spectrum of the complex exhibits ν(N=N) peak at 1404 cm⁻¹ which is lower



Scheme 1. Synthesis of dimeric rhodium(III) complex, $[\text{Rh}_2(\text{PPh}_3)_2(\text{L})_2\text{Cl}_2]$ (**1**).

than the free ligand value [36]. ¹H NMR spectrum of the complex was taken in CDCl₃. All the expected proton signals of the ligands including aromatic protons are resolved except S—CH₂CH₃ peaks, which suggests the C—S bond cleavage in the complex. A series of overlapping multiplet signals appeared in the region 7.24–8.23 ppm correspond to the protons of coordinated triphenylphosphine along with azo-thiophenolato ligand in the complex. The UV–vis spectrum of the complex in acetonitrile exhibits a low energy sharp peak at 595 nm ($\epsilon \times 10^{-3}$, 12.54 M⁻¹cm⁻¹) along with a shoulder peak at 515 nm ($\epsilon \times 10^{-3}$, 7.43 M⁻¹cm⁻¹). In addition, two ligand centered peaks appeared at 371 nm ($\epsilon \times 10^{-3}$, 16.49 M⁻¹cm⁻¹) and 320 nm ($\epsilon \times 10^{-3}$, 19.55 M⁻¹cm⁻¹) in acetonitrile (Fig. 1).

3.2. Molecular structure

Single crystals of $[\text{Rh}_2(\text{PPh}_3)_2(\text{L})_2\text{Cl}_2]$ (**1**) suitable for structure determination were grown by slow diffusion of n-hexane into dichloromethane solution of the complex. The molecular structure of **1** was unambiguously confirmed by single crystal X-ray structure analysis. The molecule is crystallized in monoclinic crystal system with *C*2/c symmetry. Detailed crystallographic information and data collection are summarized in Table 1. Selected bond lengths and bond angles of the complex are given in Table 2. The ORTEP plot of the dimeric complex is represented in Fig. 2. Each of the rhodium center of the dimeric complex has pseudo octahedral environment. The thiophenolato ligand L coordinated to Rh center through azo-N, phenolic-O and thiophenolato-S atoms. The thiophenolato-S bridges between the two rhodium centers in the dimeric complex

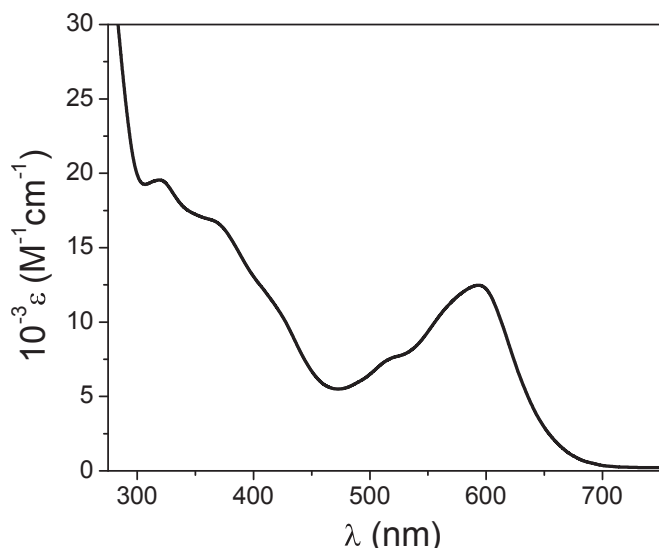


Fig. 1. UV–vis spectrum of **1** in acetonitrile.

Table 2
Selected X-ray and calculated bond distances and angles of **1**.

Bonds(Å)	X-ray	Calc.
Rh1–N1	1.956(7)	2.047
Rh1–O1	2.026(6)	2.069
Rh1–S1	2.253(3)	2.363
Rh1–P1	2.318(2)	2.408
Rh1–Cl1	2.346(2)	2.404
Rh1–S1 ⁱ	2.686(4)	2.492
S1–C1	1.761(10)	1.782
O1–C8	1.272(10)	1.286
N1–N2	1.279(8)	1.276
Angles (°)		
N1–Rh1–O1	91.4(3)	89.796
N1–Rh1–S1	87.4(2)	85.609
N1–Rh1–S1 ⁱ	87.59(19)	95.897
N1–Rh1–Cl1	175.8(2)	177.898
N1–Rh1–P1	91.32(19)	93.911
O1–Rh1–S1	173.5(2)	171.157
O1–Rh1–S1 ⁱ	93.7(2)	90.555
O1–Rh1–Cl1	87.02(17)	88.252
O1–Rh1–P1	91.2(2)	91.431
S1–Rh1–S1 ⁱ	79.95(15)	82.421
S1–Rh1–P1	95.19(12)	96.410
S1–Rh1–Cl1	93.73(10)	96.221
Rh1–S1–Rh1	99.88(15)	97.559

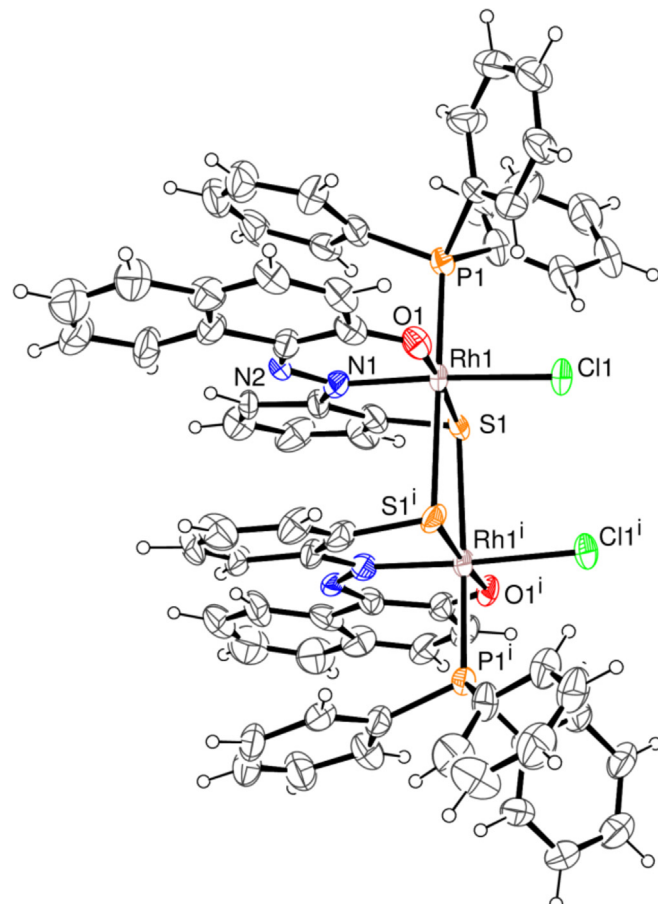


Fig. 2. ORTEP plot with 35% ellipsoidal probability of $[\text{Rh}_2(\text{PPh}_3)_2(\text{L})_2\text{Cl}_2]$ (**1**) (solvent, CH₂Cl₂ is omitted for clarity).

with Rh–S distances of 2.253(3) and 2.686(4) Å. Rh–N(azo) distance is found to be 1.956(7) Å (Rh1–N1) in the complex. The Rh–P

Table 3Energy and compositions of some selected molecular orbitals of **1**.

MO	Energy	% of composition			
		Rh	L	PPh ₃	Cl
LUMO+5	-1.06	51	38	01	10
LUMO+4	-1.12	52	30	04	13
LUMO+3	-1.66	31	40	28	01
LUMO+2	-1.81	37	38	23	3
LUMO+1	-2.30	08	87	05	0
LUMO	-2.38	06	90	03	0
HOMO	-5.07	05	86	09	0
HOMO-1	-5.23	10	86	01	03
HOMO-2	-5.42	15	08	05	72
HOMO-3	-5.70	21	35	10	34
HOMO-4	-5.73	13	35	16	36
HOMO-5	-5.74	28	23	02	47
HOMO-6	-6.07	18	56	04	23
HOMO-7	-6.10	15	34	12	39
HOMO-8	-6.24	02	78	07	13
HOMO-9	-6.28	04	77	18	01
HOMO-10	-6.39	10	55	14	21

(Rh1–P1, 2.318(2) Å) and Rh–Cl (Rh1–Cl1, 2.346(2) Å) bond distances are found as expected for other rhodium triphenylphosphine complexes [53,54]. The rhodium coordination sphere deviates from ideal octahedron and significant deviation of bond angle is detected for S1–Rh1–S1ⁱ, 79.95(15)°.

3.3. DFT and TDDFT calculations

Geometry optimization of **1** was carried out by using DFT/B3LYP method to interpret the electronic structure of the complex. The optimized bond distances and angles are well reproducing the X-

ray crystal structure data (Table 2). HOMO and HOMO-1 of the complex has 86% ligand character along with reduced contribution of $d\pi(\text{Rh})$ (5–10%). HOMO-2 has 72% $p\pi(\text{Cl})$ and 15% $d\pi(\text{Rh})$ character. HOMO-3 to HOMO-7 has mixed $d\pi(\text{Rh})$ (13–28%), $p\pi(\text{Cl})$ (23–47%) and $\pi(\text{L})$ (23–56%) character. LUMO and LUMO+1 of the complex has 87–90% $\pi^*(\text{L})$ character, while LUMO+2 to LUMO+5 has mixed contribution of $d\pi(\text{Rh})$ (31–52%) and $\pi^*(\text{L})$ (30–40%) orbitals (Table 3, Fig. 3).

To get deep insight into the electronic transition of the complex vertical electronic transitions were calculated by TDDFT method using CPCM model in acetonitrile. Calculated vertical electronic transitions of **1** are summarized in Table 4. The experimental low energy band at 595 nm corresponds to the HOMO → LUMO transition ($\lambda_{\text{calc.}} = 574$ nm) having ILCT (intra-ligand charge transfer transition) character. The band at 515 nm of the complex again has ILCT character corresponds to HOMO-1 → LUMO+1 transition ($\lambda_{\text{calc.}} = 525$ nm). The shoulder peak at 422 nm has mixed MLCT (metal to ligand charge transfer transition) and ILCT character, while the high energy peaks at 371 and 320 nm correspond to ILCT transitions in the complex.

3.4. Catalytic transfer hydrogenation reactions

The synthesized Rh(III) complex was employed as catalyst for transfer hydrogenation of ketones which is a significant and useful process in organic synthesis. The catalytic reaction conditions were optimized with respect to bases, catalyst loading and reaction time. The transfer hydrogenation of acetophenone to 1-phenylethanol was chosen as a standard reaction in *i*-PrOH. The results of transfer hydrogenation of acetophenone (2 mmol) using 0.5 mol% of complex **1** and 0.02 mmol of different bases are summarized in Table 5. In case of weak bases such as Na₂CO₃ and CH₃COONa the

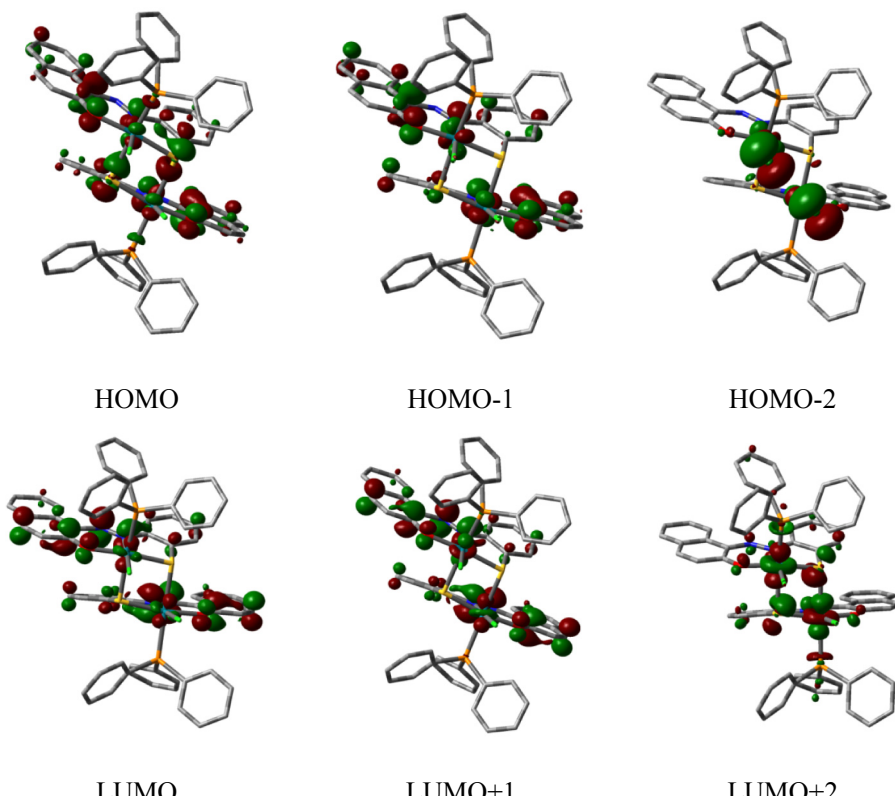
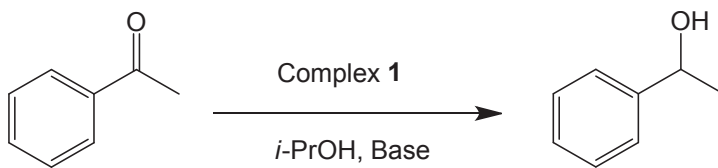


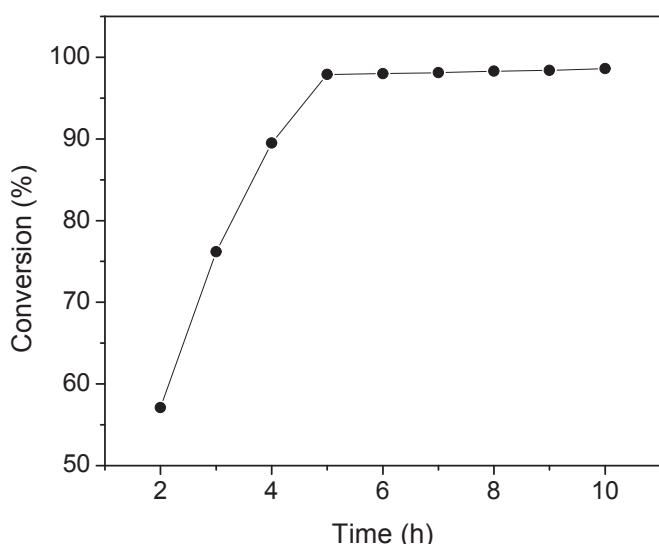
Fig. 3. Contour plots of selected molecular orbitals of $[\text{Rh}_2(\text{PPh}_3)_2(\text{L})_2\text{Cl}_2]$ (**1**). Isodensity value 0.04 e Bohr⁻³.

Table 4Vertical electronic transition calculated by TDDFT/CPCM method of **1**.

λ (nm)	E (eV)	Osc. Strength (f)	Key excitations	Character	$\lambda_{\text{expt.}}$ (nm) ($10^{-3}\epsilon, \text{M}^{-1}\text{cm}^{-1}$)
574.1	2.1598	0.2462	(95%)HOMO → LUMO	$\pi(L) \rightarrow \pi(L^*)$ ILCT	595(12.54)
525.2	2.3608	0.1319	(73%)HOMO-1 → LUMO+1	$\pi(L) \rightarrow \pi(L^*)$ ILCT	515(7.43)
432.5	2.8667	0.0634	(76%)HOMO-3 → LUMO	$d\pi(\text{Rh})/\pi(L) \rightarrow \pi(L^*)$ MLCT/ILCT	
426.2	2.9091	0.1677	(67%)HOMO-2 → LUMO+1	$d\pi(\text{Rh})/\pi(L) \rightarrow \pi(L^*)$ MLCT/ILCT	422(sh)
405.7	3.0562	0.1869	(65%)HOMO-6 → LUMO+1	$d\pi(\text{Rh})/\pi(L) \rightarrow \pi(L^*)$ MLCT/ILCT	
372.7	3.3267	0.1562	(63%)HOMO-8 → LUMO	$\pi(L) \rightarrow \pi(L^*)$ ILCT	371(16.49)
327.5	3.7860	0.2560	(61%)HOMO-9 → LUMO+1	$\pi(L) \rightarrow \pi(L^*)$ ILCT	320(19.55)

Table 5Effect of bases and reaction time on the transfer hydrogenation of acetophenone^a.

Entry	Base	Time (h)	Conversion ^b (%)
1	KOH	2	57.1
2	KOH	3	76.2
3	KOH	4	89.5
4	KOH	5	97.9
5	KOH	6	98.0
6	KOH	7	98.1
7	KOH	8	98.3
8	KOH	9	98.4
9	KOH	10	98.6
10	NaOH	5	96.3
11	Na ₂ CO ₃	5	43.8
12	CH ₃ COONa	5	37.2
13	KO <i>t</i> Bu	5	71.5

^a Reaction condition: acetophenone (2 mmol), complex **1** (0.5 mol %), catalyst:base 1:4 in *i*-PrOH (10 mL) at 80 °C.^b Conversion was determined by GC with undecane as an internal standard.**Fig. 4.** Time dependence of the catalytic transfer hydrogenation of acetophenone using 1 mol % catalyst **1** in *i*-PrOH at 80 °C with KOH as base.

conversions were significantly low (37–44%), whereas a moderate conversion was observed in case of KO*t*Bu (72%). The catalytic conversions were significantly enhanced with strong bases such as KOH or NaOH (96–98%). Hence KOH was chosen as base in all reactions. Furthermore, the catalytic conversions with different time intervals were also monitored and the maximum conversion was achieved within the 5 h of reaction (Fig. 4). To explore the efficiency of the catalyst towards transfer hydrogenation reaction, low catalyst loading test was carried out. The reactions were screened using 1.0–0.05 mol% of catalyst concentration. For 0.05 and 0.1 mol% of the catalyst loading the conversion rates were significantly dropped with high turnover numbers (TONs), while maximum conversions were achieved in minimum 0.2 mol% of the catalyst with appreciable turnover number (TON) (Table 6). So, 0.2 mol% catalyst concentration was used for all catalytic reactions.

A series of ketones were screened in transfer hydrogenation reactions using C:S ratio of 1:500 and KOH as base in *i*-PrOH. The results transfer hydrogenation of ketones are summarized in Table 7. The maximum conversion was observed for *p*-methoxyacetophenone (98%) to corresponding alcohol. The conversions of other acetophenones were found to be in the range 91–97%. Excellent catalytic conversions were also achieved for cyclic ketones such as cyclopentanone (97%), cyclohexanone (94%) and

Table 6Effect of low catalyst loading^a.

Entry	Mol % of 1	Conversion ^b (%)	TON ^c
1	1.0	98.9	99
2	0.75	98.3	131
3	0.5	97.9	196
4	0.3	97.5	325
5	0.25	97.3	389
6	0.2	97.2	486
7	0.15	83.6	557
8	0.1	72.3	723
9	0.05	47.5	950

^a Reaction condition: acetophenone (2 mmol), complex **1** (0.05–1.0 mol%), catalyst:base 1:4 in *i*-PrOH (10 mL) at 80 °C for 5 h.

^b Conversion was determined by GC with undecane as an internal standard.

^c Turnover number (TON) = mole of product/mol of catalyst.

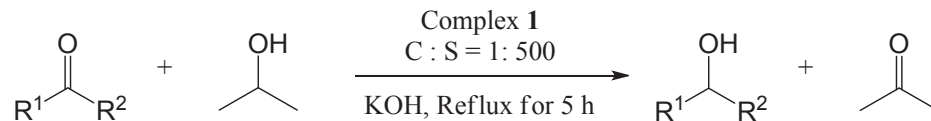
4. Conclusion

A new dimeric rhodium(III) triphenylphosphine complex, [Rh₂(PPh₃)₂(L)₂Cl₂] (**1**) is synthesized by sp³(C)–S bond cleavage of a thioether containing ligand, 1-(((2-(ethylthio)phenyl)diazetyl)methyl)naphthalen-2-ol (L-CH₂CH₃). The complex is thoroughly characterized by several spectroscopic techniques. Structure of the complex is confirmed by single crystal X-ray diffraction method. The complex exhibits excellent catalytic activity towards transfer hydrogenation of ketones in *i*-PrOH using KOH as base. Electronic structure and solution spectrum of the complex are well interpreted by DFT and TDDFT computations.

Supplementary materials

Crystallographic data for the structure of **1** has been deposited with the Cambridge Crystallographic Data center, CCDC No. 1891313. Copies of this information may be obtained free of charge from the Director, CCDC, 12 Union Road, Cambridge CB2 1EZ, UK (e-mail: deposit@ccdc.cam.ac.uk or www: <http://www.ccdc.cam.ac.uk>).

cycloheptanone (92%). Moreover, the catalytic efficiency of the present rhodium(III) complex towards transfer hydrogenation of ketones are comparable to the reported rhodium catalysts [35,55–57].

Table 7Transfer hydrogenation of ketones using complex **1**^a.

Entry	Ketones	Alcohols	Conversion (%) ^b	TON ^c	Entry	Ketones	Alcohols	Conversion (%) ^b	TON ^c
1			97.2	486	6			90.5	453
2			94.1	471	7			92.3	462
3			95.7	479	8			97.1	486
4			95.2	476	9			94.3	472
5			97.9	490	10			91.7	459

^a Experimental condition: reactions were carried out at 80 °C, ketone (2 mmol), Rh(III) complex (0.2 mol%), KOH (0.02 mmol), *i*-PrOH (10 mL).

^b Conversions were determined by GC with undecane as an internal standard and were reported mean values of three runs.

^c Turnover number (TON) = mole of product/mol of catalyst.

Acknowledgment

Financial supports received from the Science and Engineering Research Board (SERB), New Delhi, India (File No. EEQ/2018/000266) is gratefully acknowledged. TKM is also grateful to JURUSA 2.0 program for research support. P. Roy and R. Naskar are thankful to UGC, New Delhi, India for fellowship.

References

- [1] R. Tan, D. Song, *Organometallics* 30 (2011) 1637–1645.
- [2] S. Kundu, W.W. Brennessel, W.D. Jones, *Organometallics* 30 (2011) 5147–5154.
- [3] M.R. Grochowski, T. Li, W.W. Brennessel, W.D. Jones, *J. Am. Chem. Soc.* 132 (2010) 12412–12421.
- [4] N. Yuan, T. Sheng, C. Tian, S. Hu, R. Fu, X. Wu, *Inorg. Chem. Commun.* 14 (2011) 649–653.
- [5] L. Wang, W. Hea, Z. Yu, *Chem. Soc. Rev.* 42 (2013) 599–621.
- [6] S. Acharya, P. Bandyopadhyay, P. Das, S. Biswas, A.N. Biswas, *J. Organomet. Chem.* 866 (2018) 13–20.
- [7] M. Ma, J.R. Lohman, T. Liu, B. Shen, *Proc. Natl. Acad. Sci. U. S. A.* 112 (2015) 10359–10364.
- [8] M.A. Reynolds, I.A. Guzei, R.J. Angelici, *Organometallics* 20 (2001) 1071–1078.
- [9] M.A. Reynolds, I.A. Guzei, R.J. Angelici, *J. Am. Chem. Soc.* 124 (2002) 1689–1697.
- [10] C. Alvarez-Toledo, E. Delgado, B. Donnadieu, M.A. Gomez, E. Hernandez, G. Martin, F. Ortega-Jimenez, F. Zamora, *Eur. J. Inorg. Chem.* (2003) 562–568.
- [11] C.A. Tolman, *J. Am. Chem. Soc.* 92 (1970) 2956–2965.
- [12] C.A. Tolman, *Chem. Rev.* 77 (1977) 313–348.
- [13] T. Ganguly, A. Das, A. Majumdar, xxxx, *Inorg. Chem.* (2019), <https://doi.org/10.1021/acs.inorgchem.9b01144>. xxxx-xxxx.
- [14] M. Jana, A. Majumdar, *Inorg. Chem.* 57 (2018) 617–632.
- [15] N. Pal, A. Majumdar, *Inorg. Chem.* 55 (2016) 3181–3191.
- [16] Y. Uetake, T. Niwa, T. Hosoya, *Org. Lett.* 18 (2016) 2758–2761.
- [17] F. Pan, H. Wang, P.-X. Shen, J. Zhao, Z.-J. Shi, *Chem. Sci.* 4 (2013) 1573–1577.
- [18] Z. Zhang, L.S. Liebeskind, *Org. Lett.* 8 (2006) 4331–4333.
- [19] H. Yang, H. Li, R. Wittemberg, M. Egi, W. Huang, L.S. Liebeskind, *J. Am. Chem. Soc.* 129 (2007) 1132–1140.
- [20] H. Li, H. Yang, L.S. Liebeskind, *Org. Lett.* 10 (2008) 4375–4378.
- [21] H. Meerwein, R. Schmidt, *Liebigs Ann. Chem.* 444 (1925) 221–238.
- [22] W. Ponndorf, *Angew. Chem.* 39 (1926) 138–143.
- [23] A. Verley, *Bull. Soc. Chim.* 37 (1925) 537–542.
- [24] Y.M.Y. Haddad, H.B. Henbest, J. Husband, T.R.B. Mitchell, *Proc. Chem. Soc.* (1964) 361–365.
- [25] R.L. Chowdhury, J.-E. Bäckvall, *Chem. Soc. Chem. Commun.* 16 (1991) 1063–1064.
- [26] J. Ito, H. Nishiyama, *Tetrahedron Lett.* 55 (2014) 3133–3146.
- [27] R. Malacea, R. Poli, E. Manoury, *Coord. Chem. Rev.* 254 (2010) 729–752.
- [28] R. Patchett, I. Magpantay, L. Sudan, C. Schotes, A. Mezzetti, F. Santoro, *Angew. Chem. Int. Ed.* 52 (2013) 10352–10355.
- [29] W.J. Ye, M. Zhao, Z.K. Yu, *Chem. Eur. J.* 18 (2012) 10843–10846.
- [30] J. Li, Y. Ma, Z. Wang, Q. Liu, G.A. Solan, Y. Ma, W.-H. Sun, *Dalton Trans.* 47 (2018) 8738–8745.
- [31] O. Altan, M.K. Yilmaz, *J. Organomet. Chem.* 861 (2018) 252–262.
- [32] S. Biswas, D. Sarkar, P. Roy, T.K. Mondal, *Polyhedron* 131 (2017) 1–7.
- [33] S. Biswas, D. Sarkar, S. Kundu, P. Roy, T.K. Mondal, *J. Mol. Struct.* 1099 (2015) 297–303.
- [34] S. Biswas, P. Roy, S. Jana, T.K. Mondal, *J. Organomet. Chem.* 846 (2017) 201–207.
- [35] P. Roy, C.K. Manna, R. Naskar, T.K. Mondal, *Polyhedron* 158 (2019) 208–214.
- [36] S. Acharya, A. Kejriwal, A.N. Biswas, P. Das, D.N. Neogi, P. Bandyopadhyay, *Polyhedron* 38 (2018) 50–57.
- [37] S. Acharya, A. Kejriwal, A.N. Biswas, P. Das, D.N. Neogi, P. Bandyopadhyay, *Inorg. Chim. Acta* 394 (2013) 757–764.
- [38] S. Acharya, P. Bandyopadhyay, P. Das, S. Biswas, A.N. Biswas, *J. Organomet. Chem.* 866 (2018) 13–20.
- [39] SHELLXS97, G.M. Sheldrick, *SHELXS97, Programs for Crystal Structure Analysis (Release 97-2)*, University of Göttingen: Göttingen, Germany, 1997.
- [40] A.D. Becke, *J. Chem. Phys.* 98 (1993) 5648–5652.
- [41] C. Lee, W. Yang, R.G. Parr, *Phys. Rev. B* 37 (1988) 785–789.
- [42] P.J. Hay, W.R. Wadt, *J. Chem. Phys.* 82 (1985) 270–283.
- [43] W.R. Wadt, P.J. Hay, *J. Chem. Phys.* 82 (1985) 284–298.
- [44] P.J. Hay, W.R. Wadt, *J. Chem. Phys.* 82 (1985) 299–310.
- [45] R. Bauernschmitt, R. Ahlrichs, *Chem. Phys. Lett.* 256 (1996) 454–464.
- [46] R.E. Stratmann, G.E. Scuseria, M.J. Frisch, *J. Chem. Phys.* 109 (1998) 8218–8224.
- [47] M.E. Casida, C. Jamorski, K.C. Casida, D.R. Salahub, *J. Chem. Phys.* 108 (1998) 4439–4449.
- [48] V. Barone, M. Cossi, *J. Phys. Chem. A* 102 (1998) 1995–2001.
- [49] M. Cossi, V. Barone, *J. Chem. Phys.* 115 (2001) 4708–4717.
- [50] M. Cossi, N. Rega, G. Scalmani, V. Barone, *J. Comput. Chem.* 24 (2003) 669–681.
- [51] D. Oi, M.J. Frisch, G.W. Trucks, H.B. Schlegel, G.E. Scuseria, M.A. Robb, J.R. Cheeseman, G. Scalmani, V. Barone, B. Mennucci, G.A. Petersson, H. Nakatsuji, M. Caricato, X. Li, H.P. Hratchian, A.F. Izmaylov, J. Bloino, G. Zheng, J.L. Sonnenberg, M. Hada, M. Ehara, K. Toyota, R. Fukuda, J. Hasegawa, M. Ishida, T. Nakajima, Y. Honda, O. Kitao, H. Nakai, T. Vreven, J.A. Montgomery Jr., J.E. Peralta, F. Ogliaro, M. Bearpark, J.J. Heyd, E. Brothers, K.N. Kudin, V.N. Staroverov, R. Kobayashi, J. Normand, K. Raghavachari, A. Rendell, J.C. Burant, S.S. Iyengar, J. Tomasi, M. Cossi, N. Rega, J.M. Millam, M. Klene, J.E. Knox, J.B. Cross, V. Bakken, C. Adamo, J. Jaramillo, R. Gomperts, R.E. Stratmann, O. Yazyev, A.J. Austin, R. Cammi, C. Pomelli, J.W. Ochterski, R.L. Martin, K. Morokuma, V.G. Zakrzewski, G.A. Voth, P. Salvador, J.J. Dannenberg, S. Dapprich, A.D. Daniels, Ö. Farkas, J.B. Foresman, J.V. Ortiz, J. Cioslowski, D.J. Fox, Gaussian 09, Revision, Gaussian, Inc., Wallingford CT, 2009.
- [52] N.M. O'Boyle, A.L. Tenderholz, K.M. Langner, *J. Comput. Chem.* 29 (2008) 839–845.
- [53] S. Roy, S. Pramanik, T. Ghorui, S. Dinda, S.S. Patra, K. Pramanik, *New J. Chem.* 42 (2018) 5548–5555.
- [54] M. Fátima, C.G. da Silva, A.M. Trzeciak, J.J. Ziolkowski, A.J.L. Pombeiro, *J. Organomet. Chem.* 620 (2001) 174–181.
- [55] M.U. Raja, R. Ramesh, K.H. Ahn, *Tetrahedron Lett.* 50 (2009) 7014–7017.
- [56] K. Rafikova, N. Kystaubayeva, M. Aydemir, C. Kayan, Y.S. Ocak, H. Temel, A. Zazybin, N. Gürbüz, İ. Özdemir, *J. Organomet. Chem.* 758 (2014) 1–8.
- [57] M. Aydemir, N. Meric, C. Kayan, F. Ok, A. Baysal, *Inorg. Chim. Acta* 398 (2013) 1–10.